Solar Phys (2007) 246: 445–456
DOI 10.1007/s11207-007-9082-7

Magnetic Flux Imbalance of the Solar and Heliospheric Magnetic Fields

A.V. Mordvinov

Received: 10 June 2007 / Accepted: 31 October 2007 / Published online: 27 November 2007

Abstract A comparative analysis of solar and heliospheric magnetic fields in terms of their cumulative sums reveals cyclic and long-term changes that appear as a magnetic flux imbalance and alternations of dominant magnetic polarities. The global magnetic flux imbalance of the Sun manifests itself in the solar mean magnetic field (SMMF) signal. The north – south asymmetry of solar activity and the quadrupole mode of the solar magnetic field contribute the most to the observed magnetic flux imbalance. The polarity asymmetry exhibits the Hale magnetic cycle in both the radial and azimuthal components of the interplanetary magnetic field (IMF). Analysis of the cumulative sums of the IMF components clearly reveals cyclic changes in the IMF geometry. The accumulated deviations in the IMF spiral angle from its nominal value also demonstrate long-term changes resulting from a slow increase of the solar wind speed over 1965 – 2006. A predominance of the positive IMF B_z with a significant linear trend in its cumulative signal is interpreted as a manifestation of the relic magnetic field of the Sun. Long-term changes in the IMF B_z are revealed. They demonstrate decadal changes owing to the 11/22-year solar cycle. Long-duration time intervals with a dominant negative B_z component were found in temporal patterns of the cumulative sum of the IMF B_z.

Keywords Sun: magnetic field · Interplanetary magnetic field

1. Introduction

The magnetic field of the Sun has a multiscale and hierarchical structure. The solar hydromagnetic dynamo generates multipole modes of magnetic field of various symmetry properties in parallel with the dominant dipole mode (Krause and Rädler, 1980). The multipole expansion also exhibits a strong quadrupole mode (Zhao, Hoeksema, and Scherrer, 2005). The quadrupole mode oscillates mainly in phase with the dominant dipole mode (Mursula

A.V. Mordvinov (✉)
Institute of Solar-Terrestrial Physics, Russian Academy of Sciences, Siberian Branch, P.O. Box 291, Irkutsk, Russia
e-mail: avm@iszf.irk.ru

and Hiltula, 2004). The north – south asymmetry of solar magnetic activity also exhibits long-term variability (Verma, 1987).

The transition from differential to rigid rotation occurs in the tachocline region, which is studied in helioseismology (Kosovichev, Schou, and Sherrer, 1997; Schou *et al.*, 1998). A weak internal magnetic field in the radiative core of the Sun was hypothesized to explain the nature of the tachocline (Charbonneau and MacGregor, 1993). Numerical MHD modeling confirmed that even a weak ($\sim 10^{-3}$ G) poloidal field can produce the tachocline (Rüdiger and Kitchatinov, 1997; MacGregor and Charbonneau, 1999). The dipole mode of the internal hypothetical field could have a lifetime that exceeds the age of the Sun owing to the high conductivity of its radiative core (Cowling, 1945). It is possible that the relic magnetic field of the Sun was captured from the convective envelope by the radiative core of the Sun at the early stage of its evolution (Kitchatinov, Jardine, and Cameron, 2001).

Indirect evidence for the internal magnetic field of the Sun adds considerable support for its existence. The small dipolar relic magnetic field of the Sun appears to point southward, having a tilt with respect to the solar rotation axis (Bravo and Stewart, 1995). In the dynamo process, the relic field, being superimposed on the reversing poloidal magnetic field, results in stronger or weaker toroidal magnetic fields, which appear in the amplitude alternation of 11-year cycles (Pudovkin and Benevolenskaya, 1984) as well as in long-term changes in solar magnetic activity (Mursula, Usoskin, and Kovaltsov, 2001). The existence of antipodal active longitudes, where magnetic activity is concentrated, could also be caused by the nonaxisymmetric relic magnetic field (Mordvinov and Kitchatinov, 2004).

Solar magnetic activity exhibits a global asymmetry because of its nonuniform hemispheric and longitudinal distribution. Three-dimensional structures of the solar magnetic field seen in the line-of-sight component result in a substantial flux imbalance through active region areas (Choudhary, Venkatakrishnan, and Gosain, 2002). Magnetic flux, being integrated over the entire solar disk, also exhibits a detectable imbalance, manifesting itself in the solar mean magnetic field (SMMF) signal (Grigoryev and Demidov, 1987), which characterizes the rotation and evolution of the large-scale magnetic field of the Sun (Mordvinov and Plyusnina, 2000).

Much of heliospheric magnetic field is rooted in unipolar background photospheric field, coronal holes, magnetic plages, and decaying active regions (Schrijver and DeRosa, 2003). The global asymmetry of solar magnetic activity also causes the magnetic imbalance of the heliospheric magnetic field. *In situ* measurements by *Ulysses* during its rapid transit showed a 10% asymmetry, with the magnetic field strength at the south pole stronger than that at the north one. A possible consequence of the north – south asymmetry of the solar magnetic field is the southward shift of the heliospheric current sheet (Smith *et al.*, 2000; Mursula and Hiltula, 2003, 2004; Zhao, Hoeksema, and Scherrer, 2005). Polarity imbalance is an inherent property of the interplanetary magnetic field (IMF) sector structure. Mursula and Hiltula (2003, 2004) revealed a regular alternation of dominant magnetic polarity in each solar hemisphere from one cycle to another. The net effect of the solar magnetic imbalance appears in cyclic and long-term changes of dominant IMF polarity (Mordvinov, 2006).

Long-term changes in the heliosphere manifest themselves in variations of the dynamic pressure of solar wind (Veselovsky *et al.*, 1999) as well as in an increase of geomagnetic activity over the past century (Lockwood, Stamper, and Wild, 1999), although its real amplitude and even existence are questioned (Mursula, Martini, and Karinen, 2004; Svalgaard and Cliver, 2005). Changes in the IMF geometry could also contribute to geomagnetic activity owing to the influence of the IMF components affecting the Earth's magnetic field. Smith and Bieber (1991) demonstrated that the IMF winding angle deviates from its mean value of 45° by up to 10°. Long-term changes of the IMF geometry cause a modulation of

galactic cosmic rays (Koudriavtsev *et al.*, 2003). The study of the long-term variability of the Sun is of great importance because of its influence on the heliosphere and on the Earth's climate (Haigh, Lockwood, and Giampapa, 2004).

The behavior of the IMF component perpendicular to the plane of the solar equator is of special interest, since it determines the geomagnetic effect of the solar wind. Both cyclic and long-term patterns in the imbalance of the IMF B_z component have been revealed (Mordvinov, 2006). These changes are of crucial importance for geomagnetic activity. The IMF B_z component near the Earth depends on many physical factors (Chao and Chen, 2001; Schwenn, 2006, and references therein). First, the B_z component is partially determined by local magnetic fields of the Sun that are carried out by the solar wind. Second, as the solar magnetic field moves away it is sometimes dramatically transformed by its interaction with the interplanetary medium. Lyatsky, Tan, and Lyatskaya (2003) revealed a significant correlation between IMF B_z and its radial component B_x, which changes its sign during the sequential activity minima in 1985 – 1987 and 1995 – 1997. An appreciable correlation exists within the activity minima under relatively quiet conditions in the solar wind. The correlation between the IMF components depends on the IMF orientation and the Sun's magnetic field polarity. The correlation between IMF B_z and $|B_x|$ is positive when the poloidal magnetic field has a positive polarity at the north pole. The correlation becomes negative after reversing of the polar magnetic field in a successive solar cycle. Because of this time-dependent correlation the Sun's magnetic field polarity generates cyclic changes in IMF B_z. A statistical study of IMF B_z also revealed a weak cyclic B_z variation owing to the direct contribution of the solar polar field, which reverses from cycle to cycle (Obridko, Golyshev, and Levitin, 2004).

In this paper long-term changes of solar and heliospheric magnetic fields are studied by analyzing their magnetic flux imbalance. A contribution of the global solar magnetic field to the IMF B_z component is demonstrated. A possible accumulated effect of the relic magnetic field of the Sun on the IMF B_z component is revealed. Changes in the radial and azimuthal IMF components also reveal changes in the IMF geometry.

2. Magnetic Flux Imbalance in the SMMF Signal

The SMMF time series was analyzed to study the nature of the full-disk magnetic flux imbalance. In fact, the SMMF signal quantifies the difference between the fluxes of positive and negative magnetic polarities of the line-of-sight component over the visible solar hemisphere (Kotov, 2006). Figures 1a and 1b depict the SMMF series S from the Wilcox Solar Observatory (Hoeksema and Scherrer, 1986) and its cumulative sum $\sum S$. The cumulative sum of the SMMF is the sum of a current value of the time series and all the previous terms. The cumulative sum reveals long-term changes in magnetic flux imbalance: a dominant positive polarity results in an increase of the cumulative sum, whereas a negative one results in its decrease. The $\sum S$ increased over 1975 – 1982, then after the polarity reversal in cycle 21 it decreased by 1992. After the polarity reversal in cycle 22 the cumulative sum decreased slowly by 1997. In cycle 23 the cumulative sum tends to rise, with its cyclic maximum in 2002. Thus, the cumulative sum of the SMMF time series exhibits the Hale magnetic cycle. As the cycle progressed the cumulative sum decreased by 6.24 mT between their consecutive maxima in 1982.5 and 2002.9.

It is reasonable to study whether the north – south asymmetry of magnetic activity and the quadrupole mode of the large-scale magnetic field of the Sun contribute to the flux imbalance of the SMMF signal. To quantify their possible contributions to $\sum S$, we estimated the fluxes

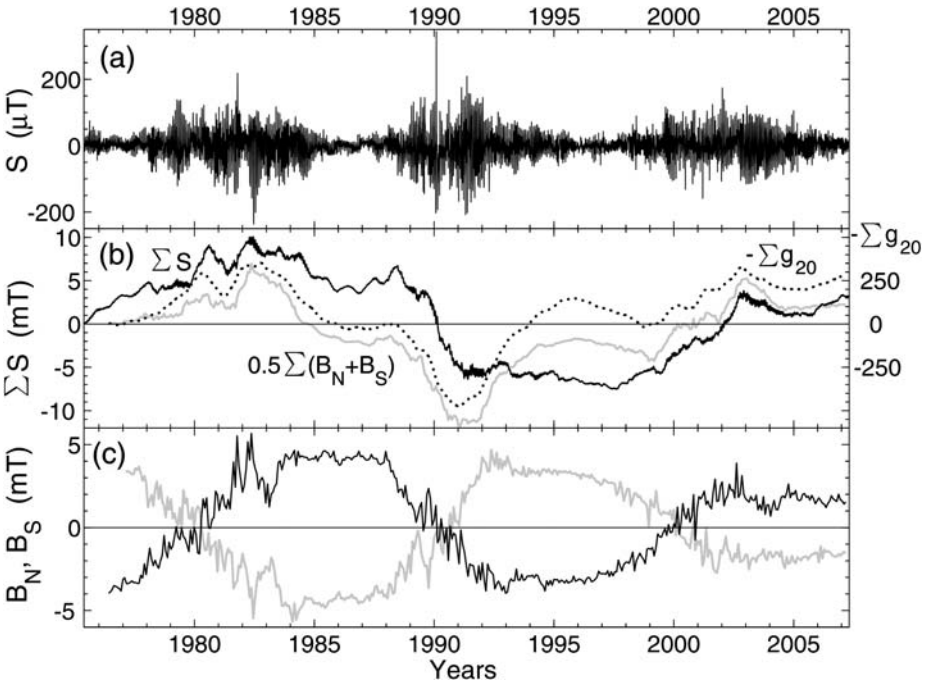

Figure 1 (a) The SMMF time series S, (b) its cumulative sum $\sum S$ (solid) compared to $0.5\sum(B_{\rm N}+B_{\rm S})$ (gray) and $\sum g_{20}$, and (c) the north (black) and south (gray) hemispheric fluxes, $B_{\rm N}$ and $B_{\rm S}$.

of the magnetic field through the source surface within the latitude zones $0°-56°$ ($B_{\rm N}$) and $-56°-0°$ ($B_{\rm S}$) separately. The fluxes of the extrapolated magnetic field at 2.5 solar radii based on the potential field model with the classic boundary conditions (Hoeksema and Scherrer, 1986) are shown in Figure 1c. The value $(B_{\rm N}+B_{\rm S})/2$ determines much of the magnetic imbalance of the SMMF signal. Its cumulative sum is shown in Figure 1b in comparison to $\sum S$.

The north–south asymmetry of magnetic activity of the Sun is partly caused by the quadrupole mode of the solar magnetic field (Mursula and Hiltula, 2004). To study their relationship we estimated the effect of the quadrupole mode as the cumulative sum of the corresponding harmonic coefficients g_{20} of the multipole expansion of the magnetic field at the source surface (Hoeksema and Scherrer, 1986). The sum $\sum g_{20}$ is also plotted in Figure 1b. This sum qualitatively agrees with both $\sum S$ and $\sum(B_{\rm N}+B_{\rm S})$, thereby suggesting their generic origin.

To verify this conclusion we have also analyzed the polar magnetic field of the Sun. The superposition of the dipole and quadrupole modes of solar magnetic field causes an asymmetry of the polar magnetic field of the Sun. The quadrupole field lines connect the Sun's poles with its equatorial region. Therefore, the imbalance of the radial component of the magnetic field at low latitudes should be in agreement with the polar field imbalance.

Figure 2a depicts magnetic field strength at the north and south poles of the Sun according to the measurements of the Wilcox Solar Observatory (Hoeksema and Scherrer, 1986). The cyclic patterns and the annual variation are well defined, the latter being caused by the Earth's excursions relative to the solar equatorial plane. The cumulative sums of the north and south polar fields are shown in Figure 2b. Annual and short-term variations are sup-

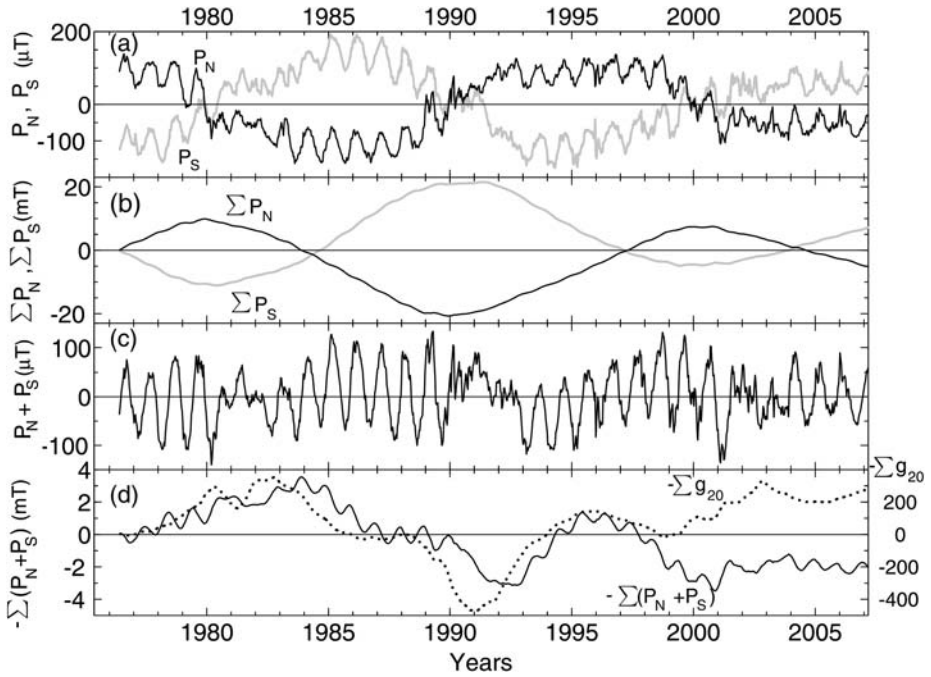

Figure 2 (a) The polar magnetic field strengths P_N and P_S and (b) their cumulative sums in comparison to (c) $P_N + P_S$ and (d) its cumulative sum and $-\sum g_{20}$.

pressed in the cumulative sum. By contrast, $\sum P_N$ and $\sum P_S$ reveal long-term changes in the polar field of the Sun. Polar field reversals occur in the epochs of the extrema of the cumulative sums. A negative polarity reverses to a positive one in 1980.4 and 1999.4 at the South pole. During this period $\sum P_S$ increases by 6.23 mT, indicating a predominance of a positive polarity at the South pole, whereas $\sum P_N$ exhibits a small but persistent decrease between its consecutive maxima, decreasing by about −2.39 mT over 1979.9 – 2000.8.

The increments of the cumulative sums, divided by the numbers of measurements, yield some constant summands at the south and north poles, which amount to 8.9 and 3.1 μT, respectively. These weak summed magnetic fields manifest themselves as a systematic increase (decrease) of the cumulative sums of the polar field strength at the south (north) poles. According to the concept of the relic magnetic field of the Sun its dipole moment is pointing southward (Bravo and Stewart, 1995; Mursula, Usoskin, and Kovaltsov, 2001; Mordvinov, 2006, and references therein). There is an independent possibility for estimating the direction and strength of the relic field based on analysis of the cumulative sums of the polar magnetic field. Indeed, the systematic increase of the cumulative sum $\sum P_S$ and the decrease of $\sum P_N$ indicate that the persistent field is pointing southward. However, the polar magnetic field record is not of sufficient duration for us to draw a definite conclusion about its strength.

Figure 2d depicts $\sum(P_N + P_S)$, which characterizes the north – south asymmetry of the polar field. This demonstrates clearly both cyclic and long-term changes in the asymmetry. The sum $-\sum g_{20}$ is also shown in Figure 2d. Cyclic patterns of the cumulative sums are qualitatively similar for 1976 – 2000 although their similarity was somewhat disrupted over

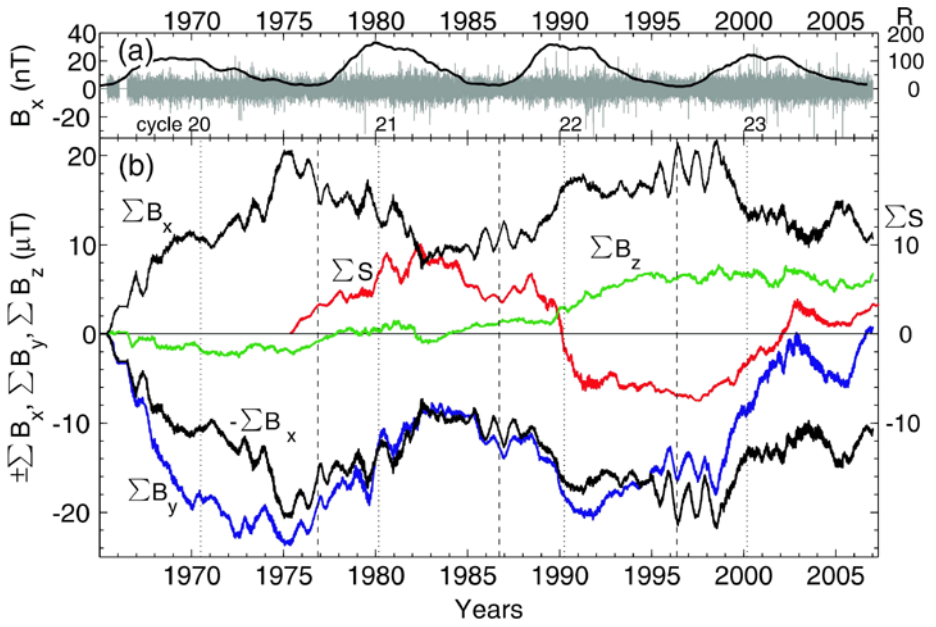

Figure 3 (a) The composite time series of hourly IMF B_x (in the GSE system) and the relative sunspot numbers; (b) the cumulative sums of the IMF components $\pm\sum B_x$, $\sum B_y$, and B_z (GSE) and $\sum S$. The sunspot minima and the reversal times of the polar magnetic field are marked with the dashed and dotted lines, respectively.

the last few years. This implies that most of the north – south asymmetry is related to the quadrupole magnetic mode of the Sun.

3. Cyclic and Long-Term Changes in the Magnetic Imbalance of the IMF

The launch of the first Soviet *Sputnik* in 1957 marked a new era in space research. Since that time multispacecraft measurements of the basic characteristics of the near-Earth environment have covered solar cycles 20 – 23. In situ IMF measurements have been collected in the space physics database OMNI2 (King and Papitashvili, 1994). The composite time series of the IMF measurements were studied in terms of their cumulative sums. The cumulative sums of the IMF components revealed the imbalance of magnetic polarities and its long-term changes (Mordvinov, 2006).

Figure 3a depicts the hourly time series of the radial IMF component B_x from the OMNI2 database and the relative sunspot numbers R throughout solar activity cycles 20 – 23. The cumulative sums of the IMF components $\pm\sum B_x$, $\sum B_y$, and $\sum B_z$ in the Geocentric Solar Ecliptic (GSE) system since 1965 are shown in Figure 3b. When estimating the cumulative sums, data in gaps were taken to be zeros. First, annual variation clearly appears in the cumulative sums of the B_x and B_y components owing to the Rosenberg and Coleman (1969) effect. Second, the Hale magnetic cycle appears in changes of the cumulative sums of the IMF B_x and B_y components owing to the alternation of dominant magnetic polarities from cycle to cycle. In fact, the cumulative sum tends to decrease in cycles 20 and 22, whereas it tends to increase over cycles 21 and 23.

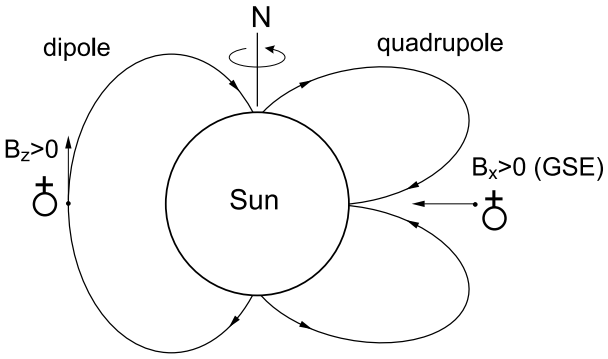

Figure 4 The dipole and quadrupole modes of the solar magnetic field contribute to the dominant IMF B_z (left) and B_x (right) components near the Earth.

The cyclic patterns of $\sum B_x$ are superimposed on a systematical increase of the cumulative sum. This increase appears clearly between the consecutive maxima or minima of the cumulative sum. The sum $\sum B_x$ increased by 1.158 μT between its consecutive minima over 1975.1 – 1998.5. It also increased by 2.4388 μT between the consecutive minima during 1982.6 – 2003.5. The systematic increase implies that a sunward polarity predominates in the near-Earth environment over the past four cycles.

Figure 3b depicts also the cumulative sum of the SMMF signal $\sum S$. There is a good qualitative agreement between temporal patterns of the solar $\sum S$ and heliospheric magnetic fields $-\sum B_x$ if we take into account the other convention for the sign of the radial component in the GSE system. Cumulative sums of the IMF components exhibit similar temporal patterns in the Geocentric Solar Equator (GSEQ) coordinate system (Mordvinov, 2006). Thus, the magnetic imbalance of the heliospheric magnetic field is due to the magnetic flux imbalance of the Sun.

The heliospheric magnetic field is an extension of the solar magnetic field. Examination of the geometry of the multipole modes of the solar large-scale magnetic field (Kuklin and Obridko, 1988; Obridko, Golyshev, and Levitin, 2004) makes it possible to explain long-term tendencies in the cumulative sums of the IMF components. Figure 4 shows the dipole and quadrupole terms of the magnetic field of the Sun and their contributions to the IMF components in the near-Earth environment. A weak dipolar relic field pointing southward at the Sun's poles has a northward component in the ecliptic plane. This persistent term superimposed on the dynamo-generated dipole results in the dominant positive-valued IMF B_z component that appears as the linear trend in its cumulative sum.

The quadrupole mode of the solar magnetic field contributes also to the observed polarity imbalance of the heliospheric magnetic field (Kuklin and Obridko, 1988). A systematic increase of $\sum B_x$ is due to a prevalence of a sunward polarity in the radial IMF component. Figure 4 also shows the specific configuration of the quadrupole mode that contributes to the IMF B_x in such a way. However, separate analysis of the cumulative sums of the IMF components does not allow us to take into account an interrelation of the IMF components. To adequately study IMF geometry we have to analyze mutual changes of the IMF components.

4. Long-Term Changes in IMF Geometry

Cyclic and long-term changes appear also in temporal patterns of the cumulative sum of the IMF azimuthal component B_y. The cumulative sum $\sum B_y$ increased by 2.886 μT between its consecutive minima (1975.1 – 1991.8) or by 7.808 μT between its maxima (1982.5 – 2002.9). The IMF azimuthal component is linked to its radial component according to the

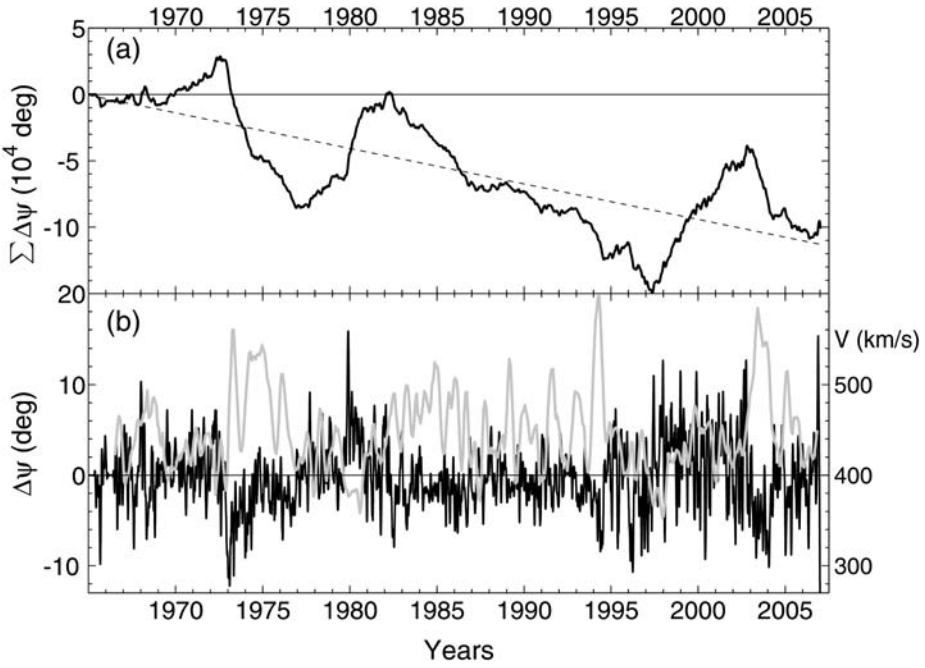

Figure 5 (a) The cumulative sum of the deviation angles $\sum \Delta\psi$ and its linear trend; (b) the instant deviation angles (black) in comparison to 27-day-averaged solar wind speed (gray).

relation that determines the spiral winding angle $\tan\psi = B_y/B_x = 2\pi r/(P \cdot V)$, where P and V are a sidereal period of rotation of the Sun and the solar wind speed at heliocentric distance r (Parker, 1958).

If the ratio between the B_x and B_y components at 1 AU were exactly constant, their cumulative sums would be directly proportional and their plots would not intersect each other. In fact, the plots of the cumulative sums $-\sum B_x$ and $\sum B_y$ cross each other several times during 1965 – 2006 in Figure 3b. Therefore, changes in the relation between the B_x and B_y components testify to changes in IMF geometry.

The mean value of the spiral winding angle is $\psi_0 = 44.9987°$ over 1965 – 2006. This value corresponds to the principal axis of the best-fit ellipse (Song and Russell, 1999) that approximates the distribution of the IMF components for the period 1965 – 2006. We calculate azimuthal deviation angles of a current tangent to the IMF spiral from its mean spiral angle $\Delta\psi = (\psi - \psi_0) \pm 180°$, $-90° \le \Delta\psi \le 90°$. The cumulative sum of the deviation angles $\sum \Delta\psi$ is shown in Figure 5a. Cyclic variations of the spiral angle are well defined in the cumulative sum of the azimuthal deviations. Then we estimate an instant spiral winding angle by taking hour-to-hour finite differences of the smoothed cumulative sum of the deviation angles $\sum \Delta\psi$. Changes in the winding angle are shown in Figure 5b in comparison to 27-day averages of the solar wind speed (King and Papitashvili, 1994). Changes in the instant deviation angle and the solar wind speed exhibit a significant anticorrelation, with the coefficient $c = -0.1984$ thereby demonstrating that high speed solar wind streams result in short-term decreases of the Parker spiral angle $\Delta\psi$.

During the phases of ascending and maximum activity, 1965 – 1972, 1977.5 – 1982.2, and 1997.4 – 2002.8, the cumulative sum of the deviation angles tends to increase, whereas it definitely decreases during phases of descending activity, 1972.6 – 1976.9, 1982.1 – 1986.8,

1993.0 – 1994.6, 1996, and 2002.8 – 2006. The amplitude of cyclic changes in $\sum \Delta\psi$ is of about 10^5 degrees for hourly data.

There are also long-term changes in the accumulated deviation angles. These appear as a systematic decrease of $\sum \Delta\psi$ that amounts to about 10^5 degrees over 1965 – 2006 for hourly data. Assuming that long-term change in the winding angle is mostly determined by the solar wind speed we estimate its integral effect using the relation $\partial\psi/\partial V = -2\pi r \cdot P/(P^2V^2 + 4\pi^2 r^2)$. The observed decrease $\sum \Delta\psi \approx 10^5$ degrees over 42 years corresponds to a slow increase in solar wind speed that amounts to about 4 km s^{-1} over this period.

5. Long-Term Changes in the IMF B_z

The north – south asymmetry in the IMF B_z component is of crucial importance for space weather conditions since large southward B_s events cause intense geomagnetic storms. Figure 6a shows the daily B_z component in the Geocentric Solar Magnetospheric (GSM) system. Any cyclic or long-term features are hardly visible in the B_z time series. However, long-term changes in the north – south B_z asymmetry are well defined in the cumulative sums of the B_z in the GSM, GSE, and GSEQ systems (Figure 6b). The cumulative sum in the GSM system characterizes the asymmetry of the IMF B_z component in reference to the Earth's magnetic field. Changes in the B_z asymmetry comprise long-term oscillations superimposed on a linear trend. A persistent increase of the cumulative sum indicates a predominance of positive-valued B_z. The least-square fitting for the IMF B_z in the GSM system displays a linear trend, which is also shown in Figure 6b. The cumulative sum of the B_z component has increased by 527 nT because of this linear trend over the past 42 years. A persistent magnetic field contributing to the cumulative sum is independent of the 11/22-year cycle.

The relic magnetic field of the Sun extended to the near-Earth environment could provide such a linear trend of the cumulative sum owing to its component perpendicular to the plane of the solar equator (Figure 4). The cumulative sums exhibit long-term deviations about the linear trend related to the cyclic reversals of the solar global magnetic field and their impacts on the IMF. When subtracting the linear trend from the cumulative sum of the B_z component, we obtain the residual cumulative sum shown in Figure 6c. Short-term fluctuations of the cumulative sum of B_z were filtered out by using a low-frequency filter.

The GSEQ coordinate system is more suitable for estimating the contribution of the relic magnetic field of the Sun to the near-Earth IMF B_z component (Mordvinov, 2006). Its strength is estimated by dividing the linear increment of the cumulative sum by the number of its measurements. The linear increment of the relic magnetic field to B_z in the GSEQ system is 776.9 nT over 42 years. According to this estimate the contribution of this stable magnetic field to the near-Earth IMF B_z component is about 0.049 ± 0.010 nT. The integral of such a weak signal is detectable by using independent in situ IMF measurements spanning the past 42 years. The error of the estimate characterizes the 95% prediction limits of the linear model, whereas the 95% confidence limits of the linear fit is ± 0.00015 nT. Although the zero drift of space-based magnetometers is expected to be below 0.1 nT over 6 months, their intrinsic sensitivity threshold is sufficient to detect the accumulated signal from the relic magnetic field of the Sun. The strength of the relic magnetic field of the Sun could be derived from its cumulative contribution to the IMF components. However, this estimate should also take into account the possible contribution of the Earth's magnetic field.

The detrended cumulative sum of the IMF B_z exhibits more or less regular excursions about its mean level on a decadal time scale. It is pertinent to compare its behavior with previous studies related to long-term changes in B_z. Lyatsky, Tan, and Lyatskaya (2003)

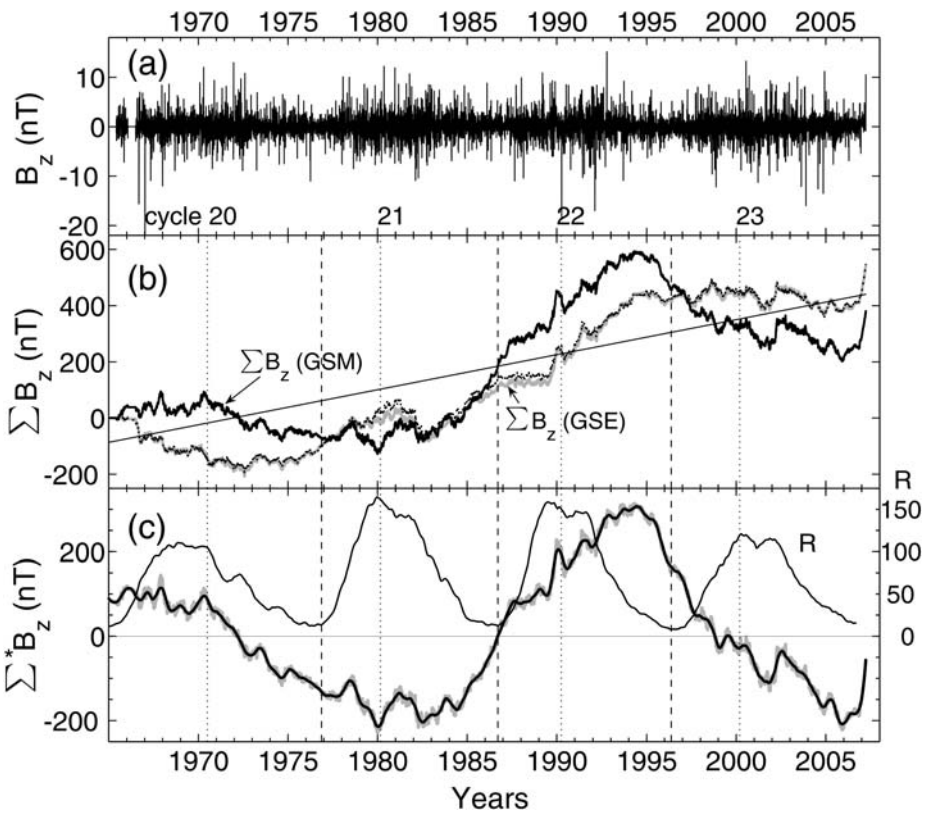

Figure 6 (a) The composite time series of daily IMF B_z in the GSM system; (b) the cumulative sums of the B_z in GSM (black), GSE (gray), and GSEQ (dotted) coordinate systems; (c) the detrended cumulative sum $\sum^* B_z$ and the sunspot numbers.

revealed that the average IMF B_z was about -1 nT during the solar minimum in 1985 – 1987 when the magnetic field at the north pole had a negative polarity, whereas it was about $+1$ nT during the minimum in 1995 – 1997 when the magnetic field at the Sun's north pole had a positive polarity. Based on the authors' analysis one could have expected a systematic decrease of $\sum B_z$ during 1985 – 1987 and its increase during 1995 – 1997. However, this is not so according to Figures 6b and 6c. The cause of this discrepancy probably involves the special selection of data for analysis, which correspond to low activity and quiet conditions in the solar wind. Assuming that the global magnetic field of the Sun determines the long-term behavior of the IMF B_z because of its connection through the near-Earth IMF, one could expect a prevalence of $B_z < 0$ in the odd 11-year cycles and a prevalence of $B_z > 0$ in the even cycles before the reversals (Obridko, Golyshev, and Levitin, 2004). Indeed, the cumulative sum of the IMF B_z tended to increase in cycle 22 and then it decreased in cycle 23. However, this is not the case for cycles 20 and 21. The cumulative sum $\sum B_z$ decreased in cycle 20 whereas it tended to increase in cycle 21. Within the 11-year cycles there were long-duration time intervals where a negative B_z component dominated. As a rule, these periods were accompanied by high geomagnetic activity (Mordvinov, 2006).

6. Conclusions

Comparative study of solar and heliospheric magnetic fields in terms of their cumulative sums reveals cyclic changes in the magnetic flux imbalance. The global magnetic flux imbalance of the Sun manifests itself in the cumulative sum of the SMMF time series. It appears in the cyclic patterns owing to the Hale cycle with a small prevalence of a sunward polarity for 1976 – 2006. The magnetic flux imbalance of the photospheric magnetic field behaves similarly to that of the extrapolated magnetic fields at the source surface and also resembles temporal changes in the quadrupole mode in terms of their cumulative sums. These findings suggest that changes in the open magnetic field of the Sun and the quadrupole mode contribute most to the observed flux imbalance.

The Hale cycle appears in the radial and azimuthal IMF components as regular cycle-to-cycle alternations of dominant polarity. A time-dependent relation between the cumulative sums of the radial and azimuthal IMF components clearly describes long-term changes in IMF geometry. Changes in solar wind speed cause cyclic deviations in the winding angle from the nominal Parker spiral. Analysis of magnetic flux imbalance makes it possible to diagnose the heliospheric magnetic field. The proposed technique, based on analysis of accumulated deviations in the IMF spiral angle from its nominal value, is also very sensitive to revealing long-term changes in IMF geometry possibly caused by a slow increase of the solar wind speed by about 4 km s^{-1} over 1965 – 2006.

Asymmetry of the solar magnetic field appears also in the IMF B_z component. Predominance of a positive-valued IMF B_z and a significant linear trend in its cumulative signal as well as the asymmetry of the polar magnetic field of the Sun were interpreted as independent evidence of the relic magnetic field of the Sun. Changes in the IMF B_z on a decadal time scale were revealed. They demonstrate a time-dependent contribution of the solar magnetic field as well as changes in IMF geometry under a solar-cycle control. Long-duration time intervals with a dominant negative B_z component were found in temporal patterns of the cumulative sum of the IMF B_z.

Acknowledgements Long-term measurements of solar and heliospheric magnetic fields used in this paper were obtained from solar and space physics databases of WSO, NASA/NSSDC, NOAA/NGDC, and SIDC. The work was supported by program No. 16 of the Presidium of the Russian Academy of Sciences, the program of state support for leading scientific schools NS-4741.2006.2, and the Russian Foundation for Basic Research (Project No. 05-02-16326a). The author is grateful to the referee for many useful suggestions and also thanks Ms. J. Sutton for improving the English version of the manuscript.

References

Bravo, S., Stewart, G.: 1995, *Astrophys. J.* **446**, 431.
Chao, J.K., Chen, H.H.: 2001, In: Song, P., *et al.* (eds.) *Space Weather, American Geophysical Union Monograph* **125**, Washington, 109.
Charbonneau, P., MacGregor, K.B.: 1993, *Astrophys. J.* **417**, 762.
Choudhary, D.P., Venkatakrishnan, P., Gosain, S.: 2002, *Astrophys. J.* **573**, 851.
Cowling, T.G.: 1945, *Mon. Not. Roy. Astron. Soc.* **105**, 167.
Grigoryev, V.M., Demidov, M.L.: 1987, *Solar Phys.* **114**, 147.
Haigh, J.D., Lockwood, M., Giampapa, V.C.: 2004, *The Sun, Solar Analogs and the Climate*, Springer, New York.
Hoeksema, J.T., Scherrer, P.H.: 1986, Solar magnetic fields – 1976 through 1985. UAG Report 94, Boulder, http://sun.stanford.wso.
King, J.H., Papitashvili, N.E.: 1994, *Interplanetary Medium Data, Suppl. 5*, National Space Science Data Center, Greenbelt, http://nssdc.gsfc.nasa.gov.
Kitchatinov, L.L., Jardine, M., Cameron, A.C.: 2001, *Astron. Astrophys.* **374**, 250.

Kosovichev, A.G., Schou, J., Sherrer, P.H.: 1997, *Solar Phys.* **170**, 43.
Kotov, V.A.: 2006, *Solar Phys.* **239**, 461.
Koudriavtsev, I.V., Kocharov, G.E., Ogurtsov, M.G., Jungner, H.: 2003, *Solar Phys.* **215**, 385.
Krause, F., Rädler, K.H.: 1980, *Mean-Field Magnetohydrodynamics and Dynamo Theory*, Pergamon, Oxford.
Kuklin, G.V., Obridko, V.N.: 1988, *Physics of Solar Activity*, Nauka, Moscow, 146.
Lockwood, M., Stamper, R., Wild, M.N.: 1999, *Nature* **399**, 437.
Lyatsky, W., Tan, A., Lyatskaya, S.: 2003, *Geophys. Res. Lett.* **30**, 24.
MacGregor, K.B., Charbonneau, P.: 1999, *Astrophys. J.* **519**, 911.
Mordvinov, A.V.: 2006, *Astron. Rep.* **50**, 936.
Mordvinov, A.V., Kitchatinov, L.L.: 2004, *Astron. Rep.* **48**, 254.
Mordvinov, A.V., Plyusnina, L.A.: 2000, *Solar Phys.* **197**, 1.
Mursula, K., Hiltula, T.: 2003, *Geophys. Res. Lett.* **30**, 22.
Mursula, K., Hiltula, T.: 2004, *Solar Phys.* **224**, 133.
Mursula, K., Martini, D., Karinen, A.: 2004, *Solar Phys.* **224**, 85.
Mursula, K., Usoskin, I.G., Kovaltsov, G.A.: 2001, *Solar Phys.* **198**, 51.
Obridko, V.N., Golyshev, S.A., Levitin, F.E.: 2004, *Geomagn. Aeron.* **44**, 410.
Parker, E.N.: 1958, *Astrophys. J.* **128**, 664.
Pudovkin, M.I., Benevolenskaya, E.E.: 1984, *Astron. Rep.* **28**, 458.
Rosenberg, R.L., Coleman, P.J.: 1969, *J. Geophys. Res.* **74**, 5611.
Rüdiger, G., Kitchatinov, L.L.: 1997, *Astron. Nachr.* **318**, 273.
Schou, J., Antia, H.M., Basu, S., Bogart, R.S., Bush, R.I., Chitre, S.M., *et al.*: 1998, *Astrophys. J.* **505**, 390.
Schrijver, C.J., DeRosa, M.L.: 2003, *Solar Phys.* **212**, 165.
Schwenn, R.: 2006, *Living Rev. Solar Phys.* **3**, 2, http: //www.livingreviews.org/lrsp-2006-2.
Smith, E.J., Jokipii, J.R., Kota, J., Lepping, R.P., Szabo, A.: 2000, *Astrophys. J.* **533**, 1084.
Smith, C.W., Bieber, J.W.: 1991, *Astrophys. J.* **370**, 435.
Song, P., Russell, C.T.: 1999, *Space Sci. Rev.* **87**, 387.
Svalgaard, L., Cliver, E.W.: 2005, *J. Geophys. Res.* **110**, A12103, doi:10.1029/ 2005JA011203.
Verma, V.K.: 1987, *Solar Phys.* **114**, 185.
Veselovsky, I.S., Dmitriev, A.V., Panasenko, O.A., Suvorova, A.V.: 1999, *Astron. Rep.* **43**, 485.
Zhao, X.P., Hoeksema, J.T., Scherrer, P.H.: 2005, *J. Geophys. Res.* **110**, A10101, doi:10.1029/ 2004JA010723.